Quantitative design of uncertain multivariable control system with an inner-feedback loop

C.-C.Cheng
Y.-K.Liao
T.-S.Wang

Indexing terms: Multivariable control systems, Inner-feedback loop, Noninteraction

Abstract: An additional inner-feedback loop is used to reduce the channel interaction of a multivariable control system such that the design of outer-feedback loop can be treated as a single-variable problem for ease in achieving the required main-channel performance. The relative error between the exact input–output relation $t_{ii}(j\omega)$ of channel i and its approximation $\hat{t}_{ii}(j\omega) = \{l_i(j\omega)f_{ii}(j\omega)\}/\{1 + l_i(j\omega)\}$ is introduced to provide an effective measure for assessing the achieved noninteraction. According to the approach proposed, the single-input/single-output quantitative-feedback-theory design method can be applied directly for the design of both inner- and outer-feedback loops.

1 Introduction

It is well known that an important reason for the use of feedback structure in control-system design is the possibility of reducing undesirable parameter-variation effects [1]. This is because many problems of practical interest appear as models with significant plant uncertainty. Typical examples include flight control and turbomachinery control over a flight envelope, as well as general automotive-engine-control problems. When multivariable feedback systems are concerned, the problems involved include the sensitivity reduction to the plant uncertainty and/or the reduction of channel interaction existing in the plant.

Among several frequency-domain techniques at present employed to solve this class of problems are the H-infinity control theory [2, 3], and the quantitative-feedback-theory (QFT) method [4, 5]. They are generally based on the single-loop configuration for practical implementation. In contrast, Kidd [6] and Yau and Nwokah [7, 8] used an additional inner-feedback loop, in the so-called internal-model-reference-loop structure, to reduce both the plant uncertainty and the channel interaction. In the latter two cases some theoretical tools, such as the direct-Nyquist-array (DNA) plot and the majorant matrix index of the compensated subsystem, were proved to be very useful for assessing the diagonal dominance achieved. It is observed that the plant-phase information is neglected in designing the inner-feedback loop, which may lead to some extent of overdesign.

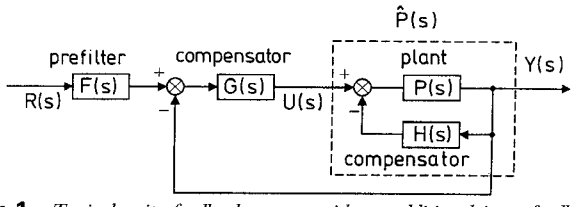

Fig. 1 *Typical unity-feedback system with an additional inner-feedback loop*

In this paper, the two-loop configuration shown in Fig. 1 is used for the design of an uncertain multi-input/multi-output (MIMO) control system. To achieve the prescribed noninteracting specification on $|\{t_{ij}(j\omega)\}/\{t_{jj}(j\omega)\}|$, a practical mechanism is provided for generating the desired inner-loop compensator. In order to treat the design of outer-feedback loop as a single-variable problem the relative error between the exact input–output relation $t_{ii}(j\omega)$ of channel i and its approximation $\hat{t}_{ii}(j\omega) = \{l_i(j\omega)f_{ii}(j\omega)\}/\{1 + l_i(j\omega)\}$ is introduced here to serve as an effective measure for assessing the achieved noninteraction of the compensated subsystem. Such a measure is proved to be relatively simple even for the system of large dimension. According to the approach proposed, the single-input/single-output (SISO) QFT design method [9] can be applied directly for the design of both inner- and outer-feedback loops.

2 Problem formulation

The considered multivariable feedback control system with two-loop configuration is shown in Fig. 1. Here $\mathbf{R}(s)$ and $\mathbf{Y}(s)$ are the n-dimensional reference input and output vectors, respectively; while $\mathbf{P}(s)$, $\mathbf{H}(s)$, $\mathbf{G}(s)$ and $\mathbf{F}(s)$ are $n \times n$ rational transfer-function matrices representing the uncertain plant, the inner-feedback compensator, the outer-feedforward compensator and the prefilter matrix, respectively. In this paper, $\mathbf{H}(s)$, $\mathbf{G}(s)$ and $\mathbf{F}(s)$ are assumed diagonal and designed to satisfy the following system requirements:

IEE Proceedings online no. 19960767

Paper first received 12th December 1995 and in revised form 8th July 1996

C.-C. Cheng is with the Institute of Electronics, National Chiao-Tung University, Hsinchu, Taiwan, Republic of China

Y.-K. Liao is with the Chung Shan Institute of Science and Technology, PO Box 90008–16–17, Lungtan, Taiwan, Republic of China

T.-S. Wang is with the Department of Control Engineering, National Chiao-Tung University, Hsinchu, Taiwan, Republic of China

(i) System noninteracting specification:

$$\left|\frac{t_{ij}(j\omega)}{t_{jj}(j\omega)}\right| \leq \lambda_{ij}\omega < 1 \quad j \neq i,\ i,j = 1,2,\ldots,n \tag{1}$$

(ii) Main-channel performance specification:

$$a_{ii}(\omega) \leq |t_{ii}(j\omega)| \leq b_{ii}(\omega) \quad i = 1,2,\ldots,n \tag{2}$$

where $t_{ij}(j\omega)$ denotes the input–output relation from channel j to i; $a_{ii}(\omega)$, $b_{ii}(\omega)$ and $\lambda_{ij}(\omega)$ are the properly prescribed positive real functions of frequency ω. In the following, the following notations are defined for convenience:

$$\mathbf{P}(s) = [p_{ij}(s)]$$
$$\mathbf{P}^{-1}(s) = \left[\frac{1}{q_{ij}(s)}\right]$$
$$\mathbf{H}(s) = \text{diag}[h_{ii}(s)]$$
$$\mathbf{G}(s) = \text{diag}[g_{ii}(s)]$$
$$\mathbf{F}(s) = \text{diag}[f_{ii}(s)]$$

The symbol diag[·] is used to indicate that the matrix [·] is diagonal.

Referring to Fig. 1, the equivalent closed inner-loop transfer-function matrix $\hat{\mathbf{P}}(s)$, from $\mathbf{U}(s)$ to $\mathbf{Y}(s)$, can be derived as

$$\hat{\mathbf{P}}(s) = [\mathbf{I} + \mathbf{P}(s)\mathbf{H}(s)]^{-1}\mathbf{P}(s) = [\mathbf{P}^{-1}(s) + \mathbf{H}(s)]^{-1}$$
$$= \begin{bmatrix} \frac{1}{q_{11}(s)}+h_{11}(s) & \frac{1}{q_{12}(s)} & \cdots & \frac{1}{q_{1n}(s)} \\ \frac{1}{q_{21}(s)} & \frac{1}{q_{22}(s)}+h_{22}(s) & \cdots & \frac{1}{q_{2n}(s)} \\ \vdots & \vdots & \ddots & \vdots \\ \frac{1}{q_{n1}(s)} & \frac{1}{q_{n2}(s)} & \cdots & \frac{1}{q_{nn}(s)}+h_{nn}(s) \end{bmatrix}^{-1}$$
$$= \begin{bmatrix} 1 & \frac{q_{11}(s)/q_{12}(s)}{1+l_{h1}(s)} & \cdots & \frac{q_{11}(s)/q_{1n}(s)}{1+l_{h1}(s)} \\ \frac{q_{22}(s)/q_{21}(s)}{1+l_{h2}(s)} & 1 & \cdots & \frac{q_{22}(s)/q_{2n}(s)}{1+l_{h2}(s)} \\ \vdots & \vdots & \ddots & \vdots \\ \frac{q_{nn}(s)/q_{n1}(s)}{1+l_{hn}(s)} & \frac{q_{nn}(s)/q_{n2}(s)}{1+l_{hn}(s)} & \cdots & 1 \end{bmatrix}^{-1}$$
$$\times \begin{bmatrix} \frac{q_{11}(s)}{1+l_{h1}(s)} & 0 & \cdots & 0 \\ 0 & \frac{q_{22}(s)}{1+l_{h2}(s)} & \cdots & 0 \\ \vdots & \vdots & \ddots & \vdots \\ 0 & 0 & \cdots & \frac{q_{nn}(s)}{1+l_{hn}(s)} \end{bmatrix}$$
$$= \gamma^{-1}(s)\hat{\mathbf{Q}}_d(s) \tag{3}$$

where

$$\gamma(s) \triangleq \begin{bmatrix} 1 & \gamma_{12}(s) & \cdots & \gamma_{1n}(s) \\ \gamma_{21}(s) & 1 & \cdots & \gamma_{2n}(s) \\ \vdots & \vdots & \ddots & \vdots \\ \gamma_{n1}(s) & \gamma_{n2}(s) & \cdots & 1 \end{bmatrix} \tag{4}$$

$$\gamma_{ij}(s) \triangleq \frac{\{q_{ii}(s)\}/\{q_{ij}(s)\}}{1 + l_{hi}(s)} \quad j \neq i,\ i,j = 1,2,\ldots,n \tag{5}$$

$$l_{hi}(s) \triangleq q_{ii}(s)h_{ii}(s) \quad i = 1,2,\ldots,n \tag{6}$$

and

$$\hat{\mathbf{Q}}_d(s) \triangleq \text{diag}[\hat{q}_{ii}(s)] = \text{diag}\left[\frac{q_{ii}(s)}{1 + l_{hi}(s)}\right] \quad i = 1,2,\ldots,n \tag{7}$$

The gain of $\{q_{ii}(j\omega)\}/\{q_{ij}(j\omega)\}$ reflects the plant coupling of channel j on channel i, which can be reduced by the inner-loop compensator.

In terms of the compensated subsystem $\hat{\mathbf{P}}(s)$, the overall closed-loop transfer-function matrix $\mathbf{T}(s) = [t_{ij}(s)]$, from $\mathbf{R}(s)$ to $\mathbf{Y}(s)$, is derived as

$$\mathbf{T}(s) = [\mathbf{I} + \hat{\mathbf{P}}(s)\mathbf{G}(s)]^{-1}\hat{\mathbf{P}}(s)\mathbf{G}(s)\mathbf{F}(s) \tag{8}$$

Substituting eqn. 3 into eqn. 8 gives

$$\mathbf{T}(s) = [\mathbf{I} + \gamma^{-1}(s)\hat{\mathbf{Q}}_d(s)\mathbf{G}(s)]^{-1}\gamma^{-1}(s)\hat{\mathbf{Q}}_d(s)\mathbf{G}(s)\mathbf{F}(s)$$
$$= [\gamma(s) + \hat{\mathbf{Q}}_d(s)\mathbf{G}(s)]^{-1}\hat{\mathbf{Q}}_d(s)\mathbf{G}(s)\mathbf{F}(s) \tag{9}$$

By defining $\mathbf{L}(s) = \text{diag}[l_i(s)] = \hat{\mathbf{Q}}_d(s)\mathbf{G}(s)$ and decomposing $\gamma(s)$ in eqn. 4 as $\gamma(s) = \mathbf{I} + \gamma_0(s)$, $\mathbf{T}(s)$ can be rewritten as

$$\mathbf{T}(s) = [\mathbf{I} + \gamma_0(s) + \mathbf{L}(s)]^{-1}\mathbf{L}(s)\mathbf{F}(s)$$
$$= [\mathbf{I} + \{I + \mathbf{L}(s)\}^{-1}\gamma_0(s)]^{-1}[\mathbf{I} + \mathbf{L}(s)]^{-1}\mathbf{L}(s)\mathbf{F}(s)$$
$$= \begin{bmatrix} 1 & \frac{\gamma_{12}(s)}{1+l_1(s)} & \cdots & \frac{\gamma_{1n}(s)}{1+l_1(s)} \\ \frac{\gamma_{21}(s)}{1+l_2(s)} & 1 & \cdots & \frac{\gamma_{2n}(s)}{1+l_2(s)} \\ \vdots & \vdots & \ddots & \vdots \\ \frac{\gamma_{n1}(s)}{1+l_n(s)} & \frac{\gamma_{n2}(s)}{1+l_n(s)} & \cdots & 1 \end{bmatrix}$$
$$\times \begin{bmatrix} \frac{l_1(s)f_{11}(s)}{1+l_1(s)} & 0 & \cdots & 0 \\ 0 & \frac{l_2(s)f_{22}(s)}{1+l_2(s)} & \cdots & 0 \\ \vdots & \vdots & \ddots & \vdots \\ 0 & 0 & \cdots & \frac{l_n(s)f_{nn}(s)}{1+l_n(s)} \end{bmatrix}$$
$$= \alpha^{-1}(s)\hat{\mathbf{T}}(s) \tag{10}$$

where

$$\alpha(s) \triangleq \begin{bmatrix} 1 & -\alpha_{12}(s) & \cdots & -\alpha_{1n}(s) \\ -\alpha_{21}(s) & 1 & \cdots & -\alpha_{2n}(s) \\ \vdots & \vdots & \ddots & \vdots \\ -\alpha_{n1}(s) & -\alpha_{n2}(s) & \cdots & 1 \end{bmatrix} \tag{11}$$

$$\alpha_{ij}(s) \triangleq \frac{-\gamma_{ij}(s)}{1 + l_i(s)} \quad j \neq i \tag{12}$$

$$l_i(s) = \hat{q}_{ii}(s)g_{ii}(s) \tag{13}$$

and

$$\hat{\mathbf{T}} \triangleq \text{diag}[\hat{t}_{ii}(s)] = \text{diag}\left[\frac{l_i(s)f_{ii}(s)}{1 + l_i(s)}\right] \quad i = 1,2,\ldots,n \tag{14}$$

In eqn. 14 it is found that, $\hat{t}_{ii}(s) = \{l_i(s)f_{ii}(s)\}/\{1 + l_i(s)\}$ possesses the familiar two-degree-of-freedom structure. If eqn. 10 is arranged as $\alpha(s)\mathbf{T}(s) = \hat{\mathbf{T}}(s)$ and both sides of it are equated,

$$\frac{t_{ij}(s)}{t_{jj}(s)} = \alpha_{ij}(s) + \sum_{k=1,k\neq i,j}^{n} \alpha_{ik}(s)\frac{t_{kj}(s)}{t_{jj}(s)}$$
$$j \neq i, \quad i,j = 1,2,\ldots,n \tag{15}$$

$$t_{ii}(s) = \hat{t}_{ii}(s) + \sum_{k=1,k\neq i}^{n} \alpha_{ik}t_{ki}(s)$$
$$i = 1,2,\ldots,n \tag{16}$$

are obtained.

Both eqns. 15 and 16 will play a key role in developing a practical synthesis procedure for achieving the prescribed system requirements of both eqns. 1 and 2.

3 Inner-feedback loop design

The design goal of the inner-feedback loop is to achieve the prescribed noninteracting specification given in eqn. 1. In the work of Cheng, Liao and Wang [10], it has been shown that, when $\alpha_{ij}(j\omega)$ in eqn. 12 is bounded by a positive-real function $\sigma_{ij}(\omega)$, i.e.

$$|\alpha_{ij}(j\omega)| = \left|\frac{-\gamma_{ij}(j\omega)}{1+l_i(j\omega)}\right| = \left|\frac{-\frac{q_{ij}(j\omega)}{q_{ij}(j\omega)} \times \frac{1}{1+l_i(j\omega)}}{1+l_{hi}(j\omega)}\right| \leq \sigma_{ij}(\omega)$$
$$j \neq i,\ i,j = 1,2,\ldots,n \tag{17}$$

with $\sigma_{ij}(\omega)$ obtained from

$$\sigma_{ij}(\omega) + \sum_{k=1,k\neq i,j}^{n} \sigma_{ik}(\omega)\lambda_{kj}(\omega) = \lambda_{ij}(\omega)$$
$$j \neq i,\ i,j = 1,2,\ldots,n \tag{18}$$

there would exist a fixed-point solution for the mapping Φ on the set **a**, which are defined as

$$\Phi : \frac{t_{ij}(j\omega)}{t_{jj}(j\omega)} \rightarrow \alpha_{ij}(j\omega) + \sum_{k=1,k\neq i,j}^{n} \alpha_{ik}(j\omega)\frac{t_{kj}(j\omega)}{t_{jj}(j\omega)}$$
$$j \neq i, \quad i,j = 1,2,\ldots,n$$

and

$$\mathbf{a} \triangleq \left\{\left|\frac{t_{ij}(j\omega)}{t_{jj}(j\omega)}\right| \text{ where } \left|\frac{t_{ij}(j\omega)}{t_{jj}(j\omega)}\right| \leq \lambda_{ij}(\omega) < 1\right.$$
$$\left. j \neq i \quad i,j = 1,2,\ldots,n\right\} \tag{19}$$

respectively. A brief interpretation of this fact is given below. First, from eqn. 19 it can be observed that, if all $\{t_{kj}(j\omega)\}/\{t_{jj}(j\omega)\}$, for $k \neq i, j$, are the members of set **a**, then

$$\left|\Phi\left\{\frac{t_{ij}(j\omega)}{t_{jj}(j\omega)}\right\}\right| \leq |\alpha_{ij}(j\omega)| + \sum_{k=1,k\neq i,j}^{n} |\alpha_{ik}(j\omega)|\left|\frac{t_{kj}(j\omega)}{t_{jj}(j\omega)}\right|$$
$$\leq \sigma_{ij}(\omega) + \sum_{k=1,k\neq i,j}^{n} \sigma_{ik}(\omega)\lambda_{kj}(\omega)$$
$$= \lambda_{ij}(\omega) \tag{20}$$

Eqn. 20 clearly points out that $\Phi\ [\{t_{ij}(j\omega)\}/\{t_{jj}(j\omega)\}]$ is also a member of set **a**. It means that $\Phi(\cdot)$ maps the set **a** into itself. By the Schauder fixed-point theorem [4], the existence of a fixed point solution for mapping Φ on set **a** is thus guaranteed.

From above statement, it is seen that both eqns. 17 and 18 provide a practical mechanism to design the inner-feedback loop for assuring the given noninteracting specification i.e.

$$\left|\frac{t_{ij}(j\omega)}{t_{jj}(j\omega)}\right| \leq \lambda_{ij}(\omega)$$

Therefore, two important results can be summarised:

(i) Using eqn. 18, the bound $\sigma_{ij}(\omega)$ for each $j \neq i$ can be obtained from the prescribed noninteracting bound $\lambda_{ij}(\omega)$.

(ii) With this derived $\sigma_{ij}(\omega)$, eqn. 17 becomes one constraint for generating the desired inner-loop function $l_{hi}(s)$.

4 Outer-feedback-loop design

The main concern here is to design the outer-feedback loop for achieving the main channel-performance specification of eqn. 2. Owing to the simple form of $\hat{t}_{ii}(j\omega)$ derived in eqn. 14, the equation $\hat{t}_{ii}(s) = \{l_i(s)f_{ii}(s)\}/\{1 + l_i(s)\}$ is preferred for design. To assess such a possibility, the relative error between $\hat{t}_{ii}(j\omega)$ and the exact $t_{ii}(j\omega)$ is defined as

$$\epsilon_i(j\omega) \triangleq \frac{t_{ii}(j\omega) - \hat{t}_{ii}(j\omega)}{t_{ii}(j\omega)} \tag{21}$$

It is seen that, if $\varepsilon_i(j\omega)$ can be bounded within some small value, the approximation $t_{ii}(j\omega) \cong \hat{t}_{ii}(j\omega)$ may have been obtained. In the following, a relation between this relative error and the prescribed $\lambda_{ij}(\omega)$ is explored. First, the exact expression of $\varepsilon_i(j\omega)$ is found, from eqn. 16, to be

$$\epsilon_i(j\omega) = \sum_{k=1,k\neq i}^{n} \alpha_{ik}(j\omega)\frac{t_{ki}(j\omega)}{t_{ii}(j\omega)} \tag{22}$$

Taking account of eqns. 17 and 18 gives

$$|\epsilon_i(j\omega)| \leq \sum_{k=1,k\neq i}^{n} |\alpha_{ik}(j\omega)|\left|\frac{t_{ki}(j\omega)}{t_{ii}(j\omega)}\right|$$
$$\leq \sum_{k=1,k\neq i}^{n} \sigma_{ik}(\omega)\lambda_{ki}(\omega) \triangleq E_i(\omega) \tag{23}$$

The above-defined $E_i(\omega)$ forms a possible upper bound on $\varepsilon_i(j\omega)$. It turns out that the smaller the $\lambda_{ij}(\omega)$, the smaller the $E_i(\omega)$. By allowing some small $E_i(\omega)$ between $\hat{t}_{ii}(j\omega)$ and $t_{ii}(j\omega)$, the main-channel performance can be approximately achieved by

$$a_{ii}(\omega) \leq \left|\hat{t}_{ii}(j\omega) = \frac{l_i(j\omega)f_{ii}(j\omega)}{1+l_i(j\omega)}\right| \leq b_{ii}(\omega) \tag{24}$$

The design problem now is to choose the proper compensators $g_{ii}(s)$ and $f_{ii}(s)$ to satisfy the specification of eqn. 24, subject to the equivalent plant $\hat{q}_{ii}(s)$. The SISO–QFT method [9] is preferred here to derive the satisfied $l_i(j\omega)$ and then $g_{ii}(j\omega)$.

5 Synthesis procedure and numerical example

In this Section, a practical synthesis procedure is proposed for the design of an uncertain MIMO feedback system. When using eqn. 17 to design the inner-feedback loop, the maximum value of $|\{-q_{ii}(j\omega)\}/\{q_{ij}(j\omega)\}|$ for all $j \neq i$, over the plant-uncertainty range, is preferred. Also suppose that the following two conditions are imposed on both loops;

$$\left|\frac{1}{1+l_i(j\omega)}\right| \leq \beta_i \quad i = 1,2\ldots,n \tag{25}$$

and

$$\left|\frac{1}{1+l_{hi}(j\omega)}\right| \leq \beta_{hi} \quad i = 1,2\ldots,n \tag{26}$$

respectively, which will provide the proper stability bound for each loop function in the high-frequency range. Then eqn. 17 can be modified as

$$\left|\frac{1}{1+l_{hi}(j\omega)}\right| \leq \min.\left\{\frac{\sigma_{ij}(\omega)}{\beta_i|\{-q_{ii}(j\omega)\}/\{q_{ij}(j\omega)\}|_{max}}\right.$$
$$\left.\text{for } j \neq i, j = 1,2,\ldots,n\right\} \ \omega \leq \omega_h \tag{27}$$

where ω_h is the universal high frequency behind which the feedback is not needed. From eqn. 27 it can be seen that smaller β_i will lead to less overdesign in deriving $l_{hi}(j\omega)$ but imposes a greater stability requirement on $l_i(s)$ due to eqn. 25. Thus, it is necessary to make trade-offs on the selection of β_i and/or β_{hi} between the desired stability requirement and the degree of overdesign. Based on both eqns. 26 and 27, the permitted bounds on the inner-loop function $l_{hi}(j\omega) = q_{ii}(j\omega)h_{ii}(j\omega)$ can be calculated with the aid of the rotated Nichols chart [9, 11]. With those derived permitted bounds, the classical loop-shaping technique will be used to find the satisfied $l_{hi}(s)$ and then $h_{ii}(s)$.

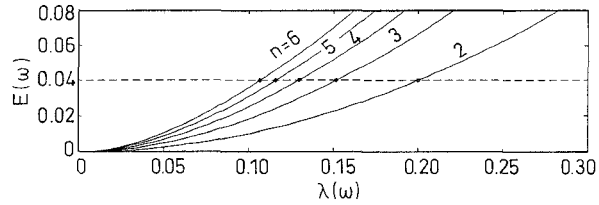

Fig. 2 *Relation of $E(\omega)$ to $\lambda(\omega)$ for $n = 2, ..., 6$*

Table 1: Data of $\lambda(\omega)$ and $\sigma(\omega)$ for $n < 6$, giving $E(\omega) = 0.04$

n	2	3	4	5	6
$\lambda(\omega)$	0.2	0.152	0.130	0.116	0.107
$\sigma(\omega)$	0.2	0.132	0.103	0.086	0.075

In designing the outer-feedback loop with respect to the specification of eqn. 24, the value of $E_i(\omega)$ should be computed to assess the possible relative error between $\hat{t}_{ii}(j\omega)$ and $t_{ii}(j\omega)$. If smaller $E_i(\omega)$ is needed, the prescribed $\lambda_{ij}(\omega)$ should be reduced. To compute $E_i(\omega)$ quickly from the given $\lambda_{ij}(\omega)$, one can consider a particular case wherein the values of $\lambda_{ij}(\omega)$ and $\sigma_{ij}(\omega)$ are chosen to be the same for all channels, respectively, i.e. $\sigma_{ij}(\omega) = \sigma(\omega)$ and $\lambda_{ij}(\omega) = \lambda(\omega)$ for all $j \neq i$. By directly replacing $\sigma_{ij}(\omega)$ and $\lambda_{ij}(\omega)$ in eqn. 18 with $\sigma(\omega)$ and $\lambda(\omega)$, respectively, the following formula is derived:

$$\sigma(\omega) = \frac{\lambda(\omega)}{1 + (n-2)\lambda(\omega)} \qquad j \neq i, \quad j = 1, 2, \ldots, n \tag{28}$$

where n is the dimension of the multivariable feedback system. For any given $\lambda(\omega)$, the corresponding $\sigma(\omega)$ is easily obtained from this formula. The $E_i(\omega)$ in eqn. 23 thus becomes

$$E_i(\omega) = \sum_{k=1, k\neq i}^{n} \sigma(\omega)\lambda(\omega) \triangleq E(\omega) \tag{29}$$

Inserting eqn. 28 into eqn. 29 yields

$$E(\omega) = \frac{(n-1)\lambda^2(\omega)}{1 + (n-2)\lambda(\omega)} \tag{30}$$

The relation of $E(\omega)$ to $\lambda(\omega)$ for $n = 2, ..., 6$ is plotted in Fig. 2. Table 1 lists some numerical data of both the corresponding $\lambda(\omega)$ and $\sigma(\omega)$, all of which result in $E(\omega) = 0.04$. The detailed synthesis procedure is as follows.

(*a*) Determination of the value of $\sigma_{ij}(\omega)$:

(i) Find the desired $\sigma_{ij}(\omega)$ from the prescribed noninteracting bound $\lambda_{ij}(\omega)$, using eqn. 18 or eqn. 28 for the particular case.

(ii) Compute the value of $E_i(\omega)$ from eqn. 23 or eqn. 30 for the particular case. if smaller $E_i(\omega)$ is needed, the designer can reduce the value of $\lambda_{ij}(\omega)$ and then repeat step (i).

(*b*) Derivation of the inner-loop function $l_{hi0}(j\omega)$ and the $h_{ii}(j\omega)$:

(i) Using the finally chosen $\sigma_{ij}(\omega)$, eqns. 26 and 27 are used as a basis on for generating the permitted bounds on the nominal inner-loop function $l_{hi0}(j\omega) = h_{ii}(j\omega)q_{i-i0}(j\omega)$ with the aid of the rotated Nichols chart [9, 11].

(ii) The desired $l_{hi0}(j\omega)$ should be shaped to sit on or above the derived permitted bounds at frequencies of interest. The compensator $h_{ii}(j\omega)$ is then obtained from the frequency data of $\{l_{hi0}(j\omega)\}/\{q_{ii0}(j\omega)\}$ using the curve-fitting method.

(*c*) Derivation of the outer-loop function $l_{i0}(j\omega)$ and the $g_{ii}(j\omega)$:

(i) The equivalent plant $\hat{q}_{ii}(s)$ is first derived according to eqn. 7, i.e. $\hat{q}_{ii}(s) = q_{ii}(s)/\{1 + l_{hi}(s)\}$. Then, based on eqns. 24 and 25, the permitted bounds on the nominal loop function $l_{i0}(j\omega) = g_{ii}(j\omega)\hat{q}_{ii0}(j\omega)$ is derived by using the SISO–QFT method directly in the Nichols chart [9, 11].

(ii) The desired $l_{i0}(j\omega)$ should be shaped to sit on or above the derived permitted bonds at frequencies of interest. The compensator $g_{ii}(j\omega)$ is then obtained from the frequency data of $\{l_{i0}(j\omega\}/\{\hat{q}_{ii0}(j\omega)\}$ using the curve-fitting method.

(*d*) Derivation of the prefilter $f_{ii}(j\omega)$:

The overall system performance is achieved by suitably choosing the prefilter $f_{ii}(j\omega)$ to shift all responses of $|l_i(j\omega)/\{1 + l_i(j\omega)\}|$ into the allowable bounds $b_{ii}(\omega)$ and $a_{ii}(\omega)$.

6 Design example

The example which will be used here to illustrate the design procedure is that previously studied by Horowitz [4]. The system to be considered consists of a 2 × 2 plant with plant transfer-function matrix

$$\mathbf{P}(s) = \begin{bmatrix} \frac{k_{11}}{1+sA_{11}} & \frac{k_{12}}{1+sA_{12}} \\ \frac{k_{21}}{1+sA_{21}} & \frac{k_{22}}{1+sA_{22}} \end{bmatrix}$$

and a total of nine plant conditions as given in Table 2.

Table 2: Nine plant conditions used in example

Plant condition	k_{11}	k_{22}	k_{12}	k_{21}	A_{11}	A_{22}	A_{12}	A_{21}
1	1	2	0.5	1	1	2	2	3
2	1	2	0.5	1	0.5	1	1	2
3	1	2	0.5	1	0.2	0.4	0.5	1
4	4	5	1	2	1	2	2	3
5	4	5	1	2	0.5	1	1	2
6	5	5	1	2	0.2	0.4	0.5	1
7	10	8	2	4	1	2	2	3
8	10	8	2	4	0.5	1	1	2
9	10	8	2	4	0.2	0.4	0.5	1

The nominal plant is taken from plant condition 1. The allowable upper and lower bounds for $|t_{ii}(j\omega)|$, i.e. $b_{ii}(\omega)$ and $a_{ii}(\omega)$, $i = 1, 2$, are given in Figs. 8 and 10.

To have proper stability margins for both loops, choose β_i = 1dB and β_{hi} = 8dB for i = 1, 2. Also choose $\lambda_{12}(\omega) = \lambda_{21}(\omega) = 0.2$ for $\omega \leq 7$ rad/s. Then, from eqn. 28, $\sigma_{12}(\omega) = \sigma_{21}(\omega) = 0.2$. The maximum relative error within this frequency range is found to be $E_1(\omega) = E_2(\omega) = 0.04$, which is acceptable in this example for the desired noninteraction capability. There is thus no need to reduce the value of $\lambda_{ij}(\omega)$. Based on eqns. 26 and 27, the permitted bounds on $l_{hi0}(j\omega)$ for i = 1, 2 are constructed in Figs. 3 and 4, respectively. The possible $lh_{i0}(s)$ are derived as

$$l_{h10}(s) = \frac{2.4(\frac{s}{72}+1)}{(\frac{s}{3}+1)(\frac{s}{18}+1)(\frac{s^2}{250^2}+\frac{s}{250}+1)}$$

$$l_{h20}(s) = \frac{4.7(\frac{s}{48}+1)}{(\frac{s}{3}+1)(\frac{s}{12}+1)(\frac{s^2}{180^2}+\frac{s}{180}+1)}$$

which are also plotted in Figs. 3 and 4. The Bode plots of $h_{ii}(j\omega)$, i = 1, 2, are shown in Fig. 5.

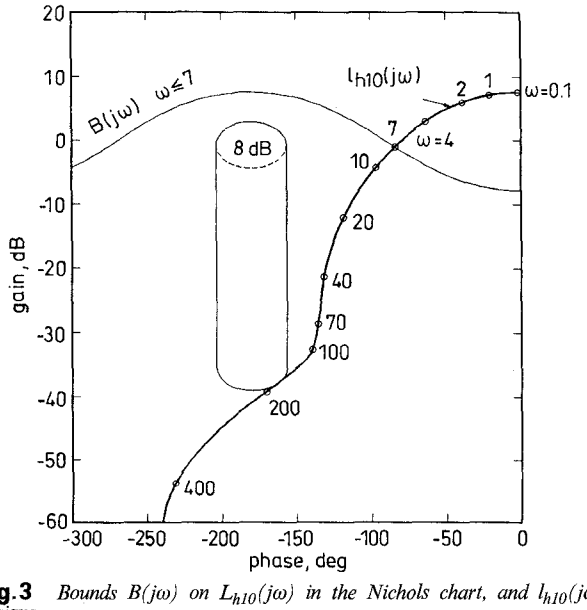

Fig.3 *Bounds $B(j\omega)$ on $L_{h10}(j\omega)$ in the Nichols chart, and $l_{h10}(j\omega)$ designs*

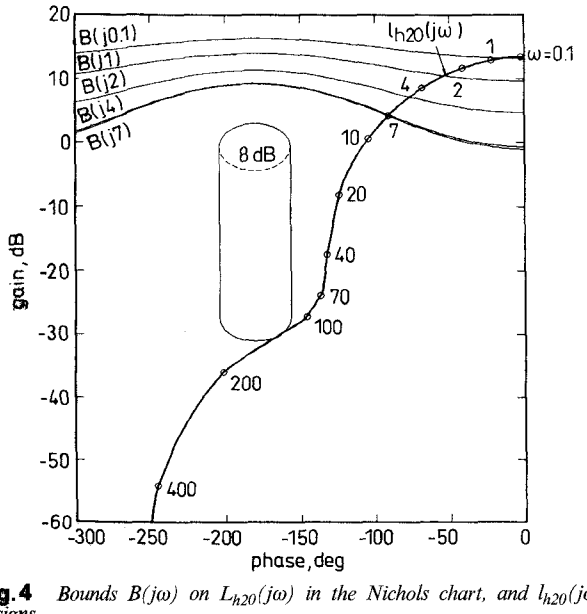

Fig.4 *Bounds $B(j\omega)$ on $L_{h20}(j\omega)$ in the Nichols chart, and $l_{h20}(j\omega)$ designs*

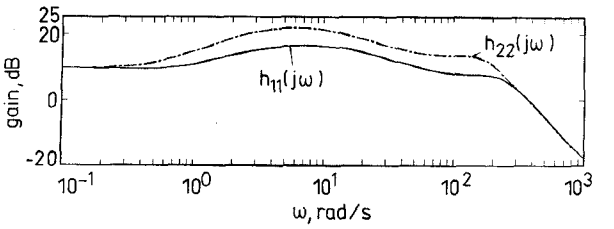

Fig.5 *Bode plots of $h_{ii}(j\omega)$ for i = 1, 2*

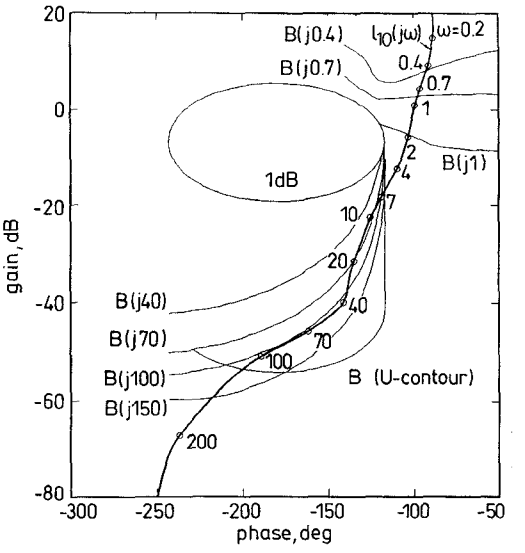

Fig.6 *Bounds $B(j\omega)$ on $l_{h10}(j\omega)$ in the Nichols chart, and $l_{h10}(j\omega)$ designs*

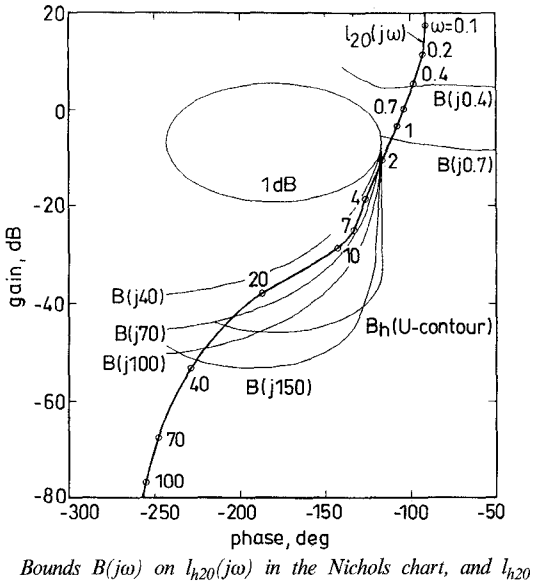

Fig.7 *Bounds $B(j\omega)$ on $l_{h20}(j\omega)$ in the Nichols chart, and $l_{h20}(j\omega)$ designs*

Now, subject to the compensated subsystem $\hat{P}(s)$, the desired $g_{ii}(s)$ and $f_{ii}(s)$ are derived using the SISO–QFT method. Based on eqns. 24 and 25, the permitted bounds on $l_{i0}(j\omega)$ for i = 1, 2 are constructed in Figs. 6 and 7, respectively. The possible $l_{i0}(s)$ are then derived as

$$l_{10}(s) = \frac{1.1(\frac{s}{20}+1)}{s(\frac{s}{7}+1)(\frac{s^2}{100^2}+\frac{1.4s}{100}+1)}$$

$$l_{20}(s) = \frac{0.75(\frac{s}{4}+1)}{s(\frac{s}{2}+1)(\frac{s^2}{20^2}+\frac{1.4s}{20}+1)}$$

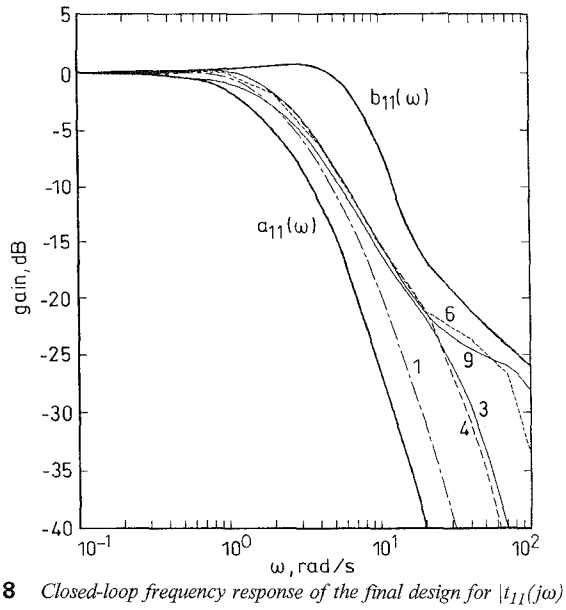

Fig. 8 *Closed-loop frequency response of the final design for* $|t_{11}(j\omega)|$

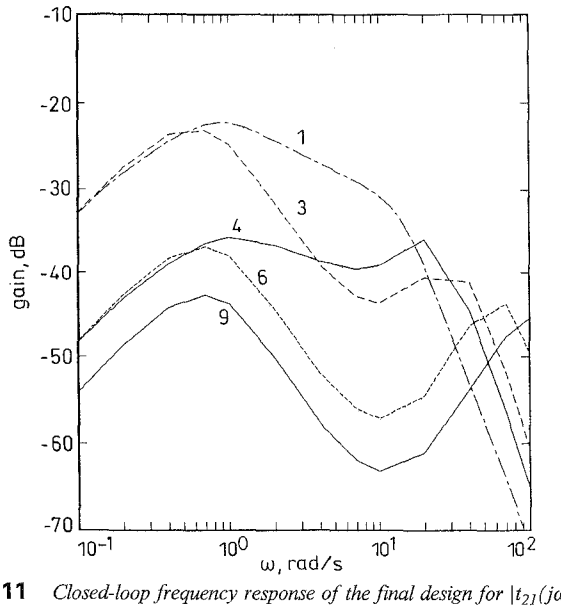

Fig. 11 *Closed-loop frequency response of the final design for* $|t_{21}(j\omega)|$

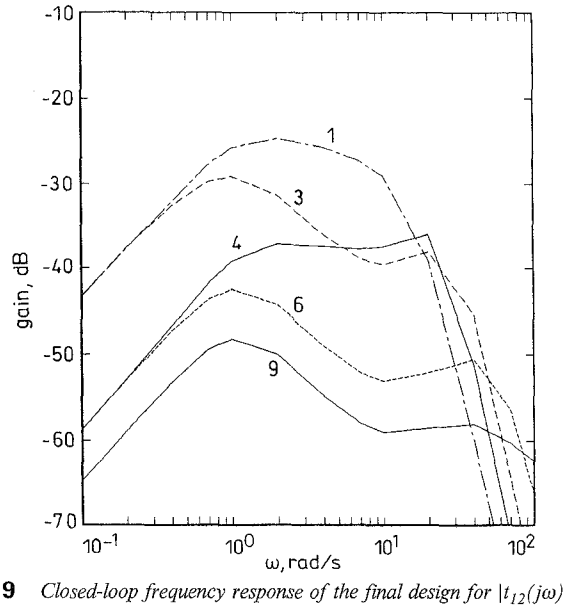

Fig. 9 *Closed-loop frequency response of the final design for* $|t_{12}(j\omega)|$

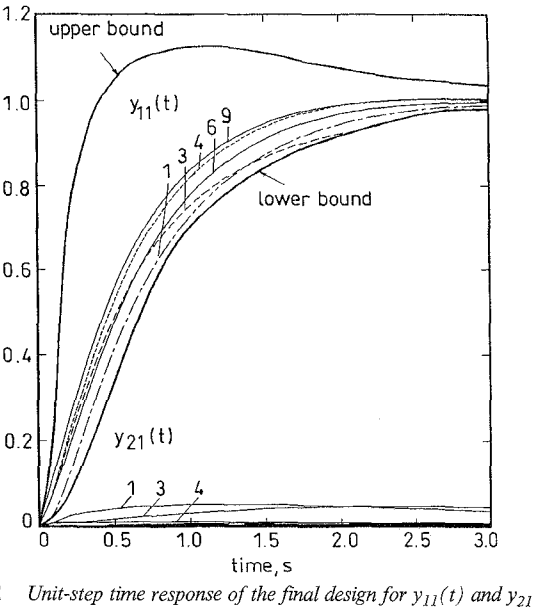

Fig. 12 *Unit-step time response of the final design for* $y_{11}(t)$ *and* $y_{21}(t)$

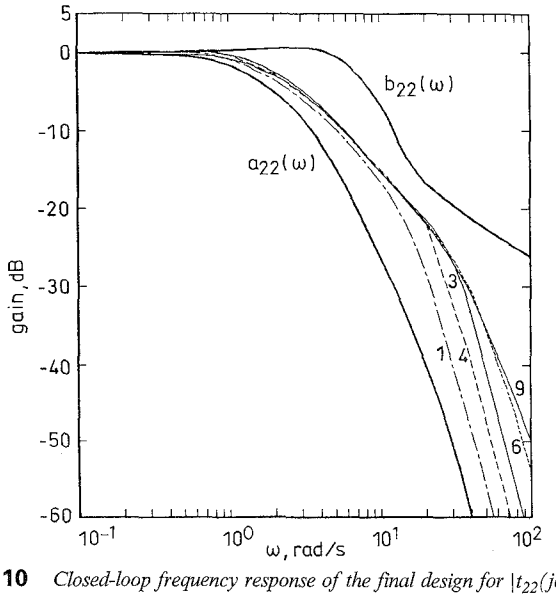

Fig. 10 *Closed-loop frequency response of the final design for* $|t_{22}(j\omega)|$

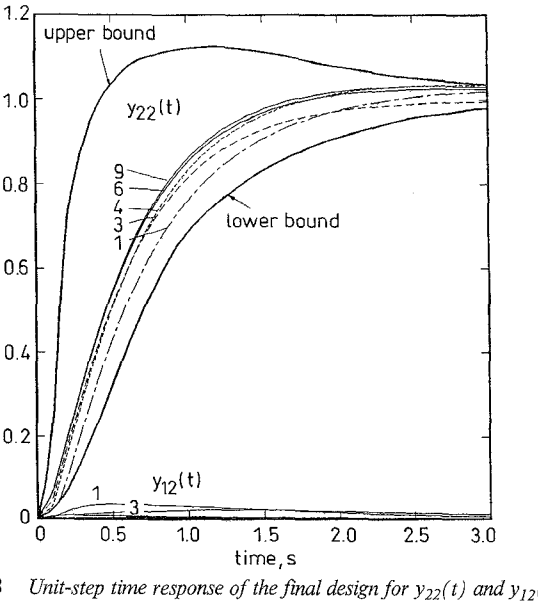

Fig. 13 *Unit-step time response of the final design for* $y_{22}(t)$ *and* $y_{12}(t)$

To achieve the overall system performance, the suitable prefilters are chosen as

$$f_{11}(s) = \frac{(\frac{s}{1.2} + 1)}{(\frac{s}{2.2} + 1)(\frac{s}{12} + 1)}$$

$$f_{22}(s) = \frac{(s + 1)}{(\frac{s}{8} + 1)^2}$$

The closed-loop frequency responses of each channel for different plant condition are shown in Figs. 8–11. The unit-step time responses of the final design are also shown in Figs. 12 and 13. All requirements are satisfied by the proposed approach.

7 Conclusion

The configuration proposed here is indeed a two-degree-of-freedom structure. During the design, the compensators $\mathbf{H}(s)$ and the $(\mathbf{G}(s), \mathbf{F}(s))$ pair are used to achieve the prescribed noninteracting specification and the main-channel-performance specification, respectively. In a practical implementation, however, a single compensator may be used to replace $\mathbf{H}(s) + \mathbf{G}(s)$ by using the curve-fitting method. In this paper, one feature of note is the use of relative error in achieving the main channel performance. According to the proposed approach, the classical frequency-domain technique can be applied directly for designing both inner- and outer-feedback loops.

8 References

1 HOROWITZ, I.M.: 'Synthesis of feedback systems' (Academic Press, Orlando, USA. 1963)

2 ZAMES, G.: 'Feedback and optimal sensitivity: model reference transformations, multiplicative semi-norms, and approximate inverses', *IEEE Trans.*, 1981, **AC–26**, pp. 301–320

3 FRANCIS, B.A.: 'A course in H∞ control theory' (Springer–Verlag, Berlin, 1987), Lecture notes in control and information sciences, Vol. 88

4 HOROWITZ, I.M.: 'Quantitative synthesis of uncertain multiple input-outputs feed-back system', *Int. J. Control*, 1979, **30**, pp. 81–106

5 HOROWITZ, I.M.: 'Improved design technique for uncertain multi-input-multi-output feedback systems', *Int. J. Control*, 1982, **36**, pp. 977–988

6 KIDD, P.T.: 'Extension of the direct Nyquist array design technique to uncertain multivariable systems subject to external disturbance', *Int. J. Control*, 1984, **40**, (5), pp. 875–901

7 YAU, C.H., and NWOKAH, O.D.I.: 'A model reference quantitative feedback design theory'. Proceedings of ASME winter annual meeting, Altanta, GA, USA, 1991, (DSC_VOL.27)

8 NWOKAH, O.D.I., and YAU, C.H.: 'Quantitative feedback design of decentralized systems', *J. Dyn. Syst. Meas. Control*, 1993, **115**, pp. 452–464

9 HOROWITZ, I.M., and SIDI, M.: 'Synthesis of feedback systems with large plant ignorance for prescribed time-domain tolerances', *Int. J. Control*, 1972, **16**, (2), pp. 287–309

10 CHENG, C.C., LIAO, Y.K., and WANG, T.S.: 'Quantitative feedback design of uncertain multivariable control systems', *Int. J. Control*, (to be published)

11 D'AZZO, J.J., and HOUPIS, C.H.: 'Linear control systems analysis and design' (McGraw–Hill, 1988), 3rd edn.